

Field emission from isolated individual vertically aligned carbon nanocones

L. R. Baylor,^{a)} V. I. Merkulov, E. D. Ellis,^{b)} M. A. Guillorn,^{b)} D. H. Lowndes, A. V. Melechko,^{c)} M. L. Simpson,^{b)} and J. H. Whealton
Oak Ridge National Laboratory, Oak Ridge, Tennessee 37831-8071

(Received 5 September 2001; accepted for publication 6 January 2002)

Field emission from isolated individual vertically aligned carbon nanocones (VACNCs) has been measured using a small-diameter moveable probe. The probe was scanned parallel to the sample plane to locate the VACNCs, and perpendicular to the sample plane to measure the emission turn-on electric field of each VACNC. Individual VACNCs can be good field emitters. The emission threshold field depends on the geometric aspect ratio (height/tip radius) of the VACNC and is lowest when a sharp tip is present. VACNCs exposed to a reactive ion etch process demonstrate a lowered emission threshold field while maintaining a similar aspect ratio. Individual VACNCs can have low emission thresholds, carry high current densities, and have long emission lifetime. This makes them very promising for various field emission applications for which deterministic placement of the emitter with submicron accuracy is needed. © 2002 American Institute of Physics.
[DOI: 10.1063/1.1455138]

I. INTRODUCTION

Carbon nanofibers (CNFs) and nanotubes (CNTs) have been shown in many studies to be candidates for use as cold cathodes for electron field emission (FE) applications.¹⁻⁴ During the past few years, prototype microelectronic devices based upon these materials also have been demonstrated.⁵⁻⁸ Vertically oriented CNFs and CNTs grown on a substrate are potentially promising FE materials due to the modest FE turn-on field that should result from a high geometric field-enhancement factor. A plasma enhanced chemical vapor deposition (PECVD) method recently was developed for growing vertically aligned CNFs (VACNFs)⁹ at relatively low ($\sim 700^\circ\text{C}$) growth temperature, which is attractive for some potential applications. The external morphology of VACNFs resembles that of multiwalled CNTs, however, from earlier transmission electron microscope (TEM) measurements, VACNFs have been found to have a different crystalline structure.¹⁰ The location of individual VACNFs is catalytically controlled in the PECVD deposition method,^{10,11} so that fabrication of FE devices based on deterministic growth of isolated VACNFs is possible.¹²

FE studies of films containing closely but randomly spaced vertically oriented CNFs and CNTs have been performed recently.^{4,13-16} However, the FE properties of individual emitters have not been determined due to their close proximity to each other in these films. In this work the FE properties of individual isolated VACNFs deterministically grown at specific locations on a substrate are measured using a moveable probe $\sim 2\ \mu\text{m}$ in diameter. The moveable probe

enables measuring the FE properties of individual VACNFs provided that they are separated sufficiently from each other such that the electric field from the probe (anode) is negligibly weak at neighboring nanofibers, thus providing data that are not available from a large nonimaging flat-plate anode as used in other recent studies.¹³⁻¹⁶ In this article, we present measurements of crucial FE parameters for individual VACNFs grown at deterministic locations, including their FE turn-on fields, maximum FE currents, and emission lifetimes.

II. EXPERIMENTAL PROCEDURE

Arrays of VACNFs were grown with $10\text{--}50\ \mu\text{m}$ spacing using a dc glow discharge PECVD process.¹⁰ The arrays were fabricated by evaporating $100\ \text{nm}$ diam catalyst dots ($\sim 10\ \text{nm}$ thick) of Ni or NiFe catalyst on an *n*-type Si wafer at the desired locations, using conventional *e*-beam lithography for patterning. The wafer had been pre-coated with a $10\ \text{nm}$ thick layer of Ti to prevent formation of Ni-silicide at elevated temperatures. Upon ammonia plasma pre-etching and heating the substrates above $\sim 600^\circ\text{C}$, the Ni dots “ball up” to form nanoscale droplets, that are the necessary precursors for the catalytic growth of a VACNF¹⁰ at each of the catalyst-dot locations. Exposure of the catalyst droplets to the PECVD process, with its vertical electric field, results in VACNF growth. The resulting isolated VACNFs are conical in shape because of the existence of separate longitudinal (internal) and lateral (external) growth mechanisms.¹⁷ They are termed vertically aligned carbon nanocones (VACNCs), in contrast to the essentially cylindrical CNFs produced within “forests” of closely spaced nanofibers.

The arrays of isolated VACNCs were imaged using a Hitachi S-4700 high-resolution field emission scanning electron microscope (SEM) with x-ray energy dispersive spectroscopy capabilities. The VACNC electron FE measurements were carried out in a high vacuum chamber (base

^{a)} Author to whom correspondence should be addressed; electronic mail: baylorlr@ornl.gov

^{b)} Also with: Dept. of Electrical and Computer Engineering, University of Tennessee.

^{c)} Also with: Center of Environmental Biotechnology, University of Tennessee.

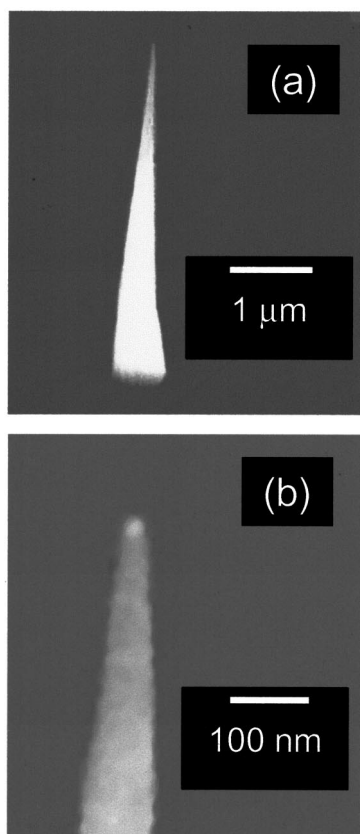


FIG. 1. SEM images of: (a) a typical individual VACNC and (b) at increased magnification showing the catalyst particle on the tip. The VACNC tip diameter is ~ 20 nm and its height is ~ 4 μm . The images were taken at 10 kV and a 45° tilt angle.

pressure $< 1 \times 10^{-6}$ Torr) by applying a positive voltage to a moveable tungsten-carbide current probe (Signatone SM-35, tip diameter of ~ 2 μm). The probe tip also was imaged with the SEM and found to be smooth on a submicron level. The translation stages for the current probe (Newport MFN25) were computer controlled with a minimum step size of 75 nm in the x - y - z directions. The distance between the probe and a point on the sample near the VACNCs was determined by contacting the substrate with the slightly biased (+10 V) probe after the FE measurements were performed. Zero height of the probe is determined when current is detected due to electrical contact. A computer-controlled Keithley 237 source-measure unit was utilized as the voltage source and current-measurement instrument. The voltage on the probe was ramped up slowly in order to avoid arcing between the probe and the VACNF under test.

III. RESULTS AND DISCUSSION

A SEM image of a typical isolated VACNC is shown in Fig. 1 where the conical shape of the carbon nanocone is clearly evident. The VACNC tip generally contains a Ni catalyst nanoparticle that is covered by a continuous thin layer (\sim several nm) of disordered carbon.¹⁰ Therefore the catalyst nanoparticles are not expected to affect the FE process to any substantial degree, and emission is presumed to come entirely from the carbon covering. Some of the VACNC arrays

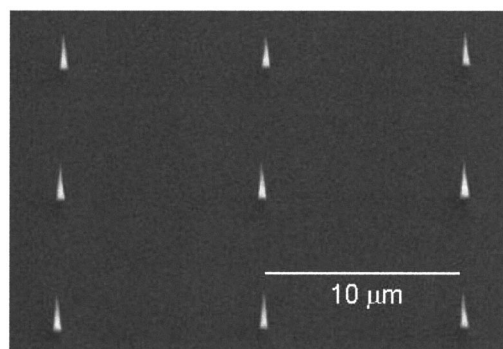


FIG. 2. A portion of an array of VACNCs with 10 μm spacing showing well isolated and uniform conically shaped nanofibers.

were exposed to a reactive ion etch (RIE) plasma using $\text{CHF}_3:\text{O}_2$ (50 sccm:2 sccm) for 10 min, in order to determine the effect of this common device-fabrication process on the nanocone structure and FE properties. The RIE process produces no discernable change in the overall VACNC shape or nanostructure of the fiber from high-resolution SEM images, although the sidewalls and any protrusions are smoothed. The catalyst nanoparticle on the VACNC tip is removed by the RIE process, thus assuring that carbon is the emitting surface.

To illustrate that FE electrons are emitted from isolated VACNCs, the probe was scanned over the arrays of nanocones, an example of which is shown in Fig. 2. An image of a probe over a typical VACNC in the configuration of the FE measurements is shown in Fig. 3. For arrays with a spacing of less than 20 μm , the FE was not clearly resolved from the individual VACNC sites because the probe produced an electric field high enough to induce FE from the nearest-neighbor VACNCs, when it was scanned at a height of 10 μm above the substrate. However, calculations of the electric field on the substrate from the probe, presented in Fig. 4, show that for 50 - μm pitch arrays the probe's electric field is

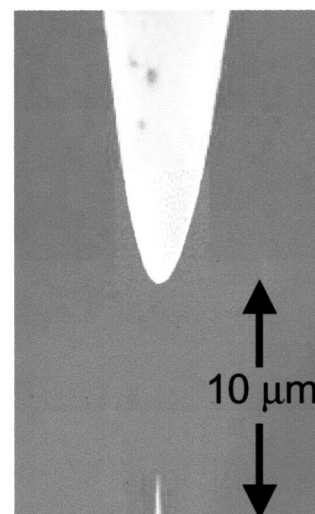


FIG. 3. Separate SEM images of the moveable probe and a VACNC combined with proper scaling to show the configuration for the measurements, with the probe at a height of 10 μm above the substrate surface.

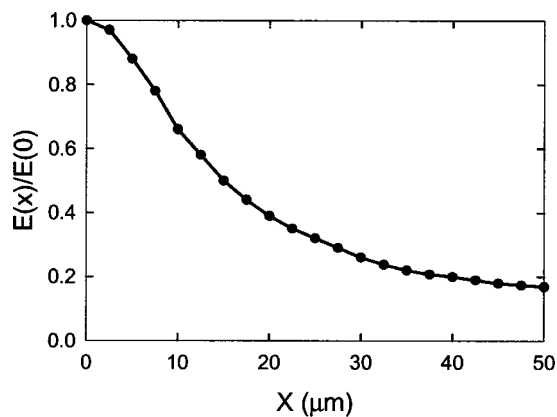


FIG. 4. A plot of the calculated electric field at the substrate as a function of the lateral distance away from the probe, for a probe height of $10 \mu\text{m}$. The field is normalized to the field directly under the probe.

nearly 1 order of magnitude lower at the neighboring nanofibers. Therefore, resolving FE from individual VACNCs with the probe is possible under these conditions. A contour plot of FE current measured during a two-dimensional (2D) raster scan of the probe across a well-isolated VACNC is presented in Fig. 5, showing that the FE is clearly localized from the individual nanocones for the $50 \mu\text{m}$ pitch arrays. The FE current from the VACNCs demonstrates Fowler–Nordheim (FN) behavior, as shown in the typical current-applied field (I – E) curve in Fig. 6.

The FE turn-on field, defined here as the macroscopic electric field needed to extract 1 nA of current, ranged from 12 to $60 \text{ V}/\mu\text{m}$ for the VACNCs studied. The aspect ratio of the VACNCs tested (defined as their height h divided by tip radius r) ranged from 150 to 700. Using the simplified FN equation,¹⁸ the expected turn-on fields are estimated to be in the range of 7–32 $\text{V}/\mu\text{m}$. These calculations assume that the entire VACNC tip is the emitting area, the work function is

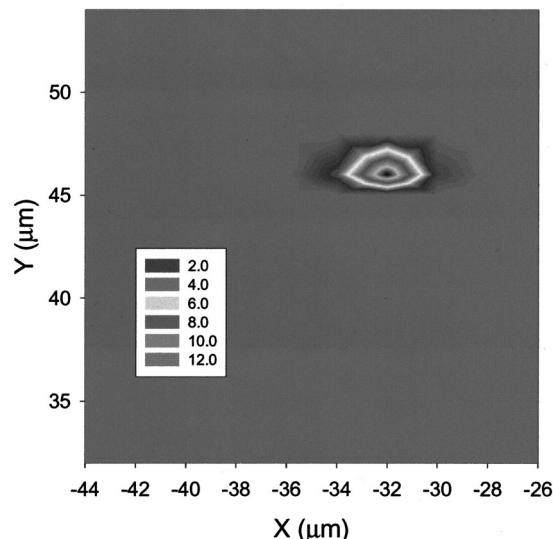


FIG. 5. Contour plot of FE current (in nA) from an isolated VACNC, measured during a raster scan of the $2 \mu\text{m}$ diam probe at a height of $10 \mu\text{m}$ above the substrate surface and biased at 300 V. The probe was scanned in discrete steps of $2 \mu\text{m}$ with a current measurement taken after each step.

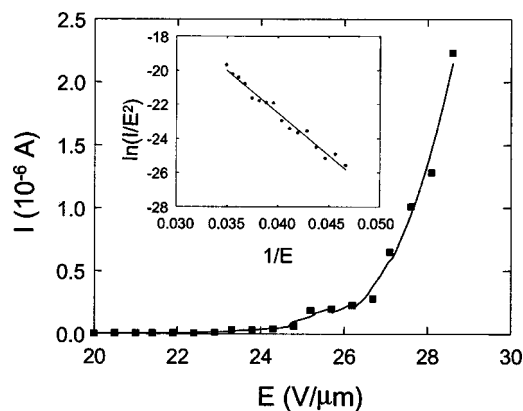


FIG. 6. Emission (I – E) curve and FN plot (inset) for an isolated VACNC. The vertical distance between the probe and the sample surface was $10 \mu\text{m}$.

that of graphite (4.6 eV), and that the geometric field enhancement factor is equal to the aspect ratio measured by SEM. A plot of the measured turn-on field as a function of measured inverse aspect ratio r/h is shown in Fig. 7. The required electric field is substantially reduced as the height is increased or tip radius is decreased, as expected due to the increased geometrical field-enhancement factor in the FN equation. The FE turn-on fields for the VACNCs that were exposed to a RIE also are shown in Fig. 4 and are generally lower than for those not exposed to a RIE. This may be due to some difficult-to-see nanoscale sharpening of the VACNC tip during the RIE process, since there was no readily observable reduction of the tip diameter as measured by high resolution SEM. A theoretical curve is included in Fig. 7 for the case of a 22 nm diam tip, typical for most of the VACNCs tested. Some of the VACNCs exposed to the RIE are very near the theoretically expected turn-on field. We note that the conical shape of the VACNCs is expected to produce a higher turn-on field than a cylindrical shape.¹⁹ This may account for the slightly higher measured turn-on fields than expected for a cylindrical emitter.

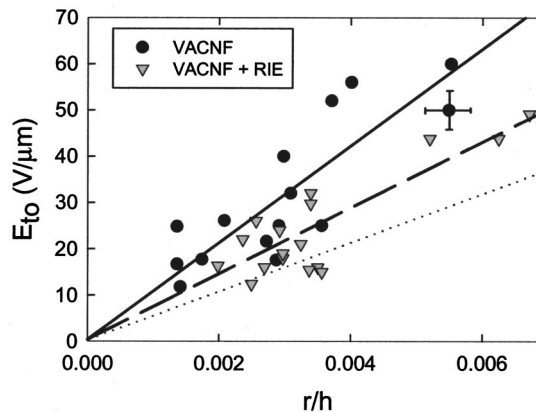


FIG. 7. Plot of VACNC turn-on electric field (for 1 nA current emission) as a function of the inverse aspect ratio (r/h). The triangle symbols are for VACNCs that were exposed to the RIE process. The lines are linear regression fits for the VACNCs before etching (solid) and after exposure to RIE (dashed). The dotted line is a theoretical calculation for a VACNC with a 11 nm tip radius.

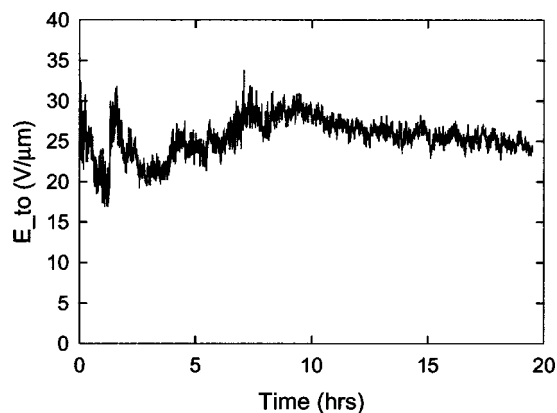


FIG. 8. Plot of the applied electric field required to maintain a 10 nA steady-state emission current from an isolated VACNC for a 20 h period.

Earlier measurements of the FE from forests of VACNFs⁴ using the same movable probe apparatus as reported here gave a lower FE threshold than expected from FN analysis. This may have been due to some undetected nanostructure on some of the VACNF tips or to high aspect ratio CNFs that were difficult to image clearly in the case of dense VACNF forests. Enhanced electron tunneling through adsorbate states²⁰ also was suggested as a possible contributing factor, but this enhancement is not observed with the isolated VACNCs.

The FE turn-on field thresholds for these isolated VACNCs are a factor of 2 or more greater than the values reported by Bonard *et al.*² for individual catalytic multi-walled nanotubes (MWNTs) and more than five times higher than reported for individual single-walled nanotubes (SWNTs). The VACNC work function is expected to be similar to that of the CNTs (~ 5 eV), therefore this difference can be largely explained by the tip diameters of the VACNCs, which are more than 15 times larger than those of the SWNTs and nearly twice that of the MWNTs in Ref. 2. These smaller diameter tips lead to larger aspect ratios and therefore higher enhancement of the electric field at the tip, which leads to lower emission thresholds. Nonetheless, the ability to grow the VACNCs in a deterministic location perpendicular to the substrate makes them very attractive for certain applications.¹² Work to reduce the VACNC tip diameter and thus the turn-on field is underway.

Stability tests of the FE from individual VACNCs have been performed and suggest that they are likely to have a long emission lifetime at expected device-operation currents, and under only moderately high vacuum conditions. One possible application for these devices is an electron source¹² for lithography operated with a constant current circuit. Therefore, a longevity test was performed in which a constant emission current of 10 nA was maintained from a typical VACNC for over 175 h (>1 week) at 1×10^{-6} Torr. A 20% decrease in the required applied field was observed over this time. A plot of the required applied field to maintain 10 nA FE is shown for a 20 h test in Fig. 8. Shorter duration constant voltage measurements were also made and show similar levels of current fluctuations. These emission lifetime results are consistent with observations of FE longevity from

films of CNTs in excess of 1000 h by Bonard *et al.*² and Murakami *et al.*¹³ and from forests of VACNFs by Merkulov *et al.*⁴

Large short-term FE currents were also measured without causing damage to the VACNC, for example 2 μ A for over 5 min. This corresponds to a current density of ~ 100 kA/cm², estimated by dividing the FE current by the VACNC tip area. This agrees well with the maximum current density obtained much earlier for individual (but much larger) carbon-fiber field emitters by Baker *et al.*¹ Other researchers have estimated the current density from vertically oriented CNT and CNF forests by dividing the measured current by the anode area.^{3,13,15} However, this underestimates current-density values since the actual emitting area is likely to be much smaller than the anode area. FE current levels of 50 μ A for short periods were found to be destructive, causing the entire VACNC to be removed from the substrate. This is presumably due to resistive heating of the VACNC or its base-to-substrate interface, or perhaps the strong electrostatic force due to field concentration at the VACNC tip.

IV. CONCLUSIONS

In conclusion, we have investigated the FE properties of isolated, deterministically grown VACNCs using a moveable current probe. Isolated VACNCs exhibit a strong dependence of the FE turn-on field on their aspect ratio, as expected from theoretical calculations.^{18,21} VACNCs with high aspect ratios have very good FE properties. Exposure of the VACNCs to RIE can further enhance their FE characteristics. This makes feasible the burial of the VACNCs in etch-compatible materials (e.g., SiO₂) for device processing. Current and future work will focus on FE imaging of controlled ordered arrays of VACNCs.

ACKNOWLEDGMENTS

The authors are grateful to the Cornell Nanofabrication Facility for providing the *e*-beam lithography and processing tools for much of this work. They also thank P. H. Fleming for assistance with sample preparation and D.T. Fehling for software development. This research was partially sponsored by the Defense Advanced Research Projects Agency (DARPA) under Contract No. DARPA-MIPR-97-1357 with Oak Ridge National Laboratory (ORNL), by the Laboratory Directed Research and Development Program of ORNL, and by the Office of Basic Energy Sciences, Division of Materials Sciences, U.S. Department of Energy. The research was carried out at ORNL, managed by UT-Battelle, LLC, for the U.S. Department of Energy under Contract No. DE-AC05-00OR22725, and in part at the Cornell Nanofabrication Facility (a member of the National Nanofabrication Users Network), which is supported by the National Science Foundation under Grant No. ECS-9731293, its users, Cornell University, and industrial affiliates.

¹F. S. Baker, A. R. Osborn, and J. Williams, *J. Phys. D* **7**, 2105 (1974).

²J.-M. Bonard, J.-P. Salvetat, T. Stockli, L. Forro, and A. Chatelain, *Appl. Phys. A: Mater. Sci. Process.* **69**, 245 (1999).

³W. Zhu, C. Bower, O. Zhou, G. Kochanski, and S. Jin, *Appl. Phys. Lett.* **75**, 873 (1999).

- ⁴V. I. Merkulov, D. H. Lowndes, and L. R. Baylor, *J. Appl. Phys.* **89**, 1933 (2001).
- ⁵Q. H. Wang, A. A. Setlur, J. M. Lauerhaas, J. Y. Dai, E. W. Seelig, and R. P. H. Chang, *Appl. Phys. Lett.* **72**, 2912 (1998).
- ⁶Y. Saito, R. Mizushima, T. Tanaka, K. Tohji, K. Uchida, M. Yumura, and S. Uemura, *Fullerene Sci. Technol.* **7**, 653 (1999).
- ⁷W. B. Choi *et al.*, *Appl. Phys. Lett.* **75**, 3129 (1999).
- ⁸Y. Lee, Y. Jang, D. Kim, J. Ahn, and B. Ju, *Adv. Mater.* **13**, 479 (2001).
- ⁹Z. F. Ren, Z. P. Huang, J. W. Xu, J. H. Wang, P. Bush, M. P. Siegal, and P. N. Provencio, *Science* **282**, 1105 (1998).
- ¹⁰V. I. Merkulov, D. H. Lowndes, Y. Y. Wei, G. Eres, and E. Voelkl, *Appl. Phys. Lett.* **76**, 3555 (2000).
- ¹¹Z. F. Ren *et al.*, *Appl. Phys. Lett.* **75**, 1086 (1999).
- ¹²M. A. Guillorn, M. L. Simpson, G. J. Bordonaro, V. I. Merkulov, L. R. Baylor, and D. H. Lowndes, *J. Vac. Sci. Technol. B* **19**, 573 (2001).
- ¹³H. Murakami, M. Hirakawa, C. Tanaka, and H. Yamakawa, *Appl. Phys. Lett.* **76**, 1776 (2000).
- ¹⁴Y. Chen, D. T. Shaw, and L. Guo, *Appl. Phys. Lett.* **76**, 2469 (2000).
- ¹⁵A. M. Rao, D. Jacques, R. C. Haddon, W. Zhu, C. Bower, and S. Jim, *Appl. Phys. Lett.* **76**, 3813 (2000).
- ¹⁶Z. H. Yuan, H. Huang, H. Y. Dang, J. E. Cao, B. H. Hu, and S. S. Fan, *Appl. Phys. Lett.* **78**, 3127 (2001).
- ¹⁷V. I. Merkulov, M. A. Guillorn, D. H. Lowndes, M. L. Simpson, and E. Voelkl, *Appl. Phys. Lett.* **79**, 1178 (2001).
- ¹⁸C. A. Spindt, I. Brodie, L. Humphrey, and E. R. Westerberg, *J. Appl. Phys.* **47**, 5248 (1976).
- ¹⁹T. Utsumi, *IEEE Trans. Electron Devices* **38**, 2276 (1991).
- ²⁰K. A. Dean, O. Groening, O. M. Kuttel, and L. Schlapbach, *Appl. Phys. Lett.* **75**, 2773 (1999).
- ²¹G. E. Vibrans, *J. Appl. Phys.* **35**, 2855 (1964).